ARTICLE OPEN

# Bcl10 is required for the development and suppressive function of Foxp3$^+$ regulatory T cells

Dandan Yang[1], Xueqiang Zhao[1] and Xin Lin[1,2]

Foxp3$^+$ regulatory T (Treg) cells play a critical role in peripheral tolerance. Bcl10, acting as a scaffolding protein in the Carma1-Bcl10-Malt1 (CBM) complex, has a critical role in TCR-induced signaling, leading to NF-κB activation and is required for T-cell activation. The role of Bcl10 in conventional T (Tconv) cells has been well characterized; however, the role of Bcl10 in the development of Treg cells and the maintenance of the suppressive function and identity of these cells has not been well characterized. In this study, we found that Bcl10 was required for not only the development but also the function of Treg cells. After deleting Bcl10 in T cells, we found that the development of Treg cells was significantly impaired. When Bcl10 was specifically deleted in mature Treg cells, the suppressive function of the Treg cells was impaired, leading to lethal autoimmunity in Bcl10$^{fl/fl}$Foxp3$^{cre}$ mice. Consistently, in contrast to WT Treg cells, Bcl10-deficient Treg cells could not protect Rag1-deficient mice from T-cell transfer-induced colitis. Furthermore, Bcl10-deficient Treg cells downregulated the expression of a series of Treg-cell effector and suppressive genes and decreased effector Treg-cell populations. Moreover, Bcl10-deficient Treg cells were converted into IFNγ-producing proinflammatory cells with increased expression of the transcription factors T-bet and HIF-1α. Together, our study results provide genetic evidence, indicating that Bcl10 is required for the development and function of Treg cells.

**Keywords:** Bcl10; Treg cells; Foxp3; autoimmune inflammation; suppressive function

*Cellular & Molecular Immunology* (2021) 18:206–218; https://doi.org/10.1038/s41423-019-0297-y

## INTRODUCTION

CD4$^+$ Foxp3$^+$ regulatory T cells (Treg cells) are a subset of T cells that play a pivotal role in maintaining self-tolerance in immune and inflammatory responses as well as immune homeostasis in different tissues.[1,2] They are composed of natural Treg cells (nTreg cells) and inducible Treg cells (iTreg cells). Natural Treg cells develop in the thymus and then transit to peripheral tissues, whereas induced Treg cells are derived from CD4$^+$ naive T cells in the periphery stimulated by cytokines such as TGFβ.[3] Treg cells express relatively high levels of the IL-2 receptor alpha chain (CD25) and the lineage defining transcription factor Foxp3.[4–7] Importantly, Foxp3 is not only an important marker of Treg cells but also a participant in the differentiation and function of Treg cells. Deficiency in Foxp3 expression leads to the ablation of Treg cells and results in lethal autoinflammatory diseases in both mice and humans.[5,6]

Functionally, mature Treg-cell populations consist of subpopulations with different differentiation patterns, resting central Tregs (cTregs) and effector Tregs (eTregs), and their suppressive functions are all controlled by signals from the T-cell antigen receptor (TCR).[8,9] cTreg cells express the homing receptor CD62L but have low expression of CD44, whereas eTreg cells highly express CD44 but lack CD62L expression. In comparison with cTregs, eTregs display an effector-like phenotype with much higher levels of proteins required for their maintenance and suppressive function, such as ICOS, KLRG1, CTLA-4, and CD44.[9–11] eTreg cells typically have a more potent immunosuppressive ability than cTregs, and reduced numbers or functional defects in the eTreg population are always linked to autoimmune disease.[9,12–14] Newly developed Treg cells in the thymus and periphery have a naive resting cTreg phenotype but can convert into eTregs after cognate Ag recognition and inflammatory factor stimulation, whereas eTregs cannot revert into cTregs.[10,11]

Treg and conventional T (Tconv) cells have antipodal physiological function even though they arise from the same progenitors in the thymus and share several similar cell-surface receptors and intracellular signaling pathways. T-cell receptor (TCR) signaling is required for Treg-cell development and Foxp3 expression, which is quite different from the signaling requirements for the development and differentiation of Tconv cells.[15–17] It remains unknown how activation of the same TCR on these two related cell types leads to such different biological phenomena, even though most of the activated molecular signaling is the same.[18] Moreover, TCR stimulation also activates transcription factors that are related to T-cell development, such as NF-κB and NFAT.[19] NF-κB is activated in response to a variety of signals, including TCR signals, has a critical role in the thymic development of Treg cells and establishes Treg-cell identity and suppressive function.[20–24]

Upon TCR activation together with CD28 costimulation in T cells, downstream events, which lead to PKCθ activation, are initiated by the tyrosine kinase ZAP70. Activated PKCθ directly phosphorylates the linker region of Carma1 (also known as

[1]Department of Basic Medical Sciences and Institute for Immunology, Tsinghua University School of Medicine, Beijing 100084, China and [2] Tsinghua University-Peking University Jointed Center for Life Sciences, Beijing 100084, China
Correspondence: Xin Lin (linxin307@tsinghua.edu.cn)

Received: 16 July 2019 Accepted: 8 September 2019
Published online: 8 October 2019

CARD11) under the control of the adaptor protein ADAP and PDK1.[25–29] The phosphorylation of CARMA1 releases its intramolecular self-inhibition state and results in CARMA1 activation.[30,31] Furthermore, activated Carma1 recruits Bcl10-Malt1 heterodimers through CARD–CARD interactions and results in prion-like polymerization of the CBM (Carma1-Bcl10-Malt1) signaling complex.[32] The assembled CBM signaling complex acts as a central scaffold to control the location of ubiquitin regulators and protein kinases, thereby leading to NF-κB and MAPK activation in T cells.[33] The CBM signaling complex has been shown to be essential for TCR signaling and has an important role in regulating the differentiation of specific T-cell subsets. Interestingly, the CBM complex is necessary for the development of thymic-derived and peripheral Treg cells under steady-state conditions.[34,35] However, the exact mechanisms by which Bcl10 regulates Treg development and function are still unclear.

In this study, we generated Bcl10-conditional knockout mice ($Bcl10^{fl/fl}$) using the CRISPR-Cas9 technique and crossed them with CD4-cre (indicated as $Bcl10^{fl/fl}$ $CD4^{cre}$) or Foxp3-YFP-cre (indicated as $Bcl10^{fl/fl}$ $Foxp3^{cre}$) mice to specifically delete Bcl10 in T cells or mature Treg cells. In $Bcl10^{fl/fl}$ $CD4^{cre}$ mice, the deletion of Bcl10 in T cells occurs during positive selection, which happens before Foxp3 expression, thereby leading to the deletion of Bcl10 in all Treg cells and resulting in an underdeveloped or missing Treg-cell population. In addition, we genetically deleted Bcl10 specifically in mature Treg cells ($Bcl10^{fl/fl}$ $Foxp3^{cre}$ mice) to investigate the roles of Bcl10 in the activation and differentiation of mature Treg cells. We found that Bcl10 regulated the suppressive function of mature Treg cells and controlled their differentiation from cTregs into eTregs. Moreover, Bcl10 deficiency in mature Treg cells resulted in their conversion from inhibitory cell types to proinflammatory cells with much higher expression of IFNγ. Together, our results indicate that Bcl10 is essential for the development and immunosuppressive function of Treg cells.

## RESULTS

### Bcl10 is required for the development of $CD4^+$ $Foxp3^+$ Treg cells

To investigate the biological function of Bcl10 in a specific cell type, we generated mice with loxP-flanked Bcl10 alleles ($Bcl10^{fl/fl}$) with CRISPR/Cas9 technology (Fig. 1a, b). We then crossed the $Bcl10^{fl/fl}$ mice with $CD4^{cre}$ mice to specifically delete Bcl10 in T cells. As expected, Bcl10 was deleted in the $Bcl10^{fl/fl}$ $CD4^{cre}$ group, and PMA/ionomycin stimulation-induced IκBα degradation was blocked in pan T cells from $Bcl10^{fl/fl}CD4^{cre}$mice (Fig. 1c). Importantly, we observed significant reductions in the proportion and absolute number of $CD4^+Foxp3^+$ Treg cells in the thymus of $Bcl10^{fl/fl}$ $CD4^{cre}$ mice compared with that of $Bcl10^{fl/+}$ $CD4^{cre}$ mice (Fig. 1d, e). Consistently, $CD4^+Foxp3^+$ Treg-cell numbers were also significantly decreased in the peripheral organs such as the spleen and lymph nodes of $Bcl10^{fl/fl}$ $CD4^{cre}$ mice compared with those of $Bcl10^{fl/+}$ $CD4^{cre}$ mice (Fig. 1f, g). These data indicate that Bcl10 is essential for the development of Treg cells both in the thymus and the peripheral organs.

To confirm this in vivo finding, we isolated $CD4^+$ naive T cells from both $Bcl10^{fl/fl}$ $CD4^{cre}$ mice and $Bcl10^{fl/+}$ $CD4^{cre}$ mice and conducted an in vitro T-cell differentiation assay. We found that Bcl10 deletion resulted in severely defective Foxp3 expression under anti-CD3/anti-CD28 antibody stimulation (Th0) or Treg-polarizing conditions (iTreg) (Fig. 1h, i), indicating that Bcl10 is also required for the differentiation of inducible Tregs (iTregs) in vitro.

### Bcl10 deficiency in Treg cells results in autoimmune inflammation

To investigate the specific function of Bcl10 in Treg cells, we crossed $Bcl10^{fl/fl}$ mice with Foxp3-cre mice to delete Bcl10 in $Foxp3^+$ cells. $Bcl10^{fl/fl}$ $Foxp3^{cre}$ mice were born at the expected Mendelian ratio. However, they developed a hunched posture and scurfy-like phenotype at ~ 14 days of life and died within 60 days (Fig. 2a, b). $Bcl10^{fl/fl}$ $Foxp3^{cre}$ mice displayed systemic inflammation with a relatively small thymus, splenomegaly, lymphadenopathy, and colitis (Fig. 2c, d). Histological analyses showed abundant infiltration of immune cells and autoinflammatory pathology in the dermis of the ears and tail and in liver, kidney, lung, and colon tissues (Fig. 2e). In addition, the levels of IgEs and proinflammatory cytokines such as TNFα, IL-6, and IL-1β were systemically increased in the serum of $Bcl10^{fl/fl}Foxp3^{cre}$ mice (Fig. 2f).

Furthermore, the percentage and number of effector $CD4^+$ and $CD8^+$ T cells in the spleen and peripheral lymph nodes were significantly increased in $Bcl10^{fl/fl}$ $Foxp3^{cre}$ mice compared with $Bcl10^{+/+}$ $Foxp3^{cre}$ mice, whereas naive $CD4^+$ and $CD8^+$ T-cell numbers were largely reduced (Fig. 3a, b, e, and f). Consistently, in the spleen and peripheral lymph nodes, IFNγ-producing $CD4^+$ and $CD8^+$ T cells were also significantly increased in both proportion and absolute number, although the percentage of $CD8^+$ cells in the lymph nodes was not increased (Fig. 3c, d, g, and h). These data suggest that Bcl10 expression in Treg cells is essential for maintaining balance in the host and immune homeostasis.

### Bcl10 is required for the suppressive function of Treg cells

Next, we investigated the suppressive function of Bcl10-deficient Treg cells in an adoptive T-cell transfer-induced colitis model in vivo. We transferred $CD45.1^+$ $CD4^+$ naive T cells alone or with WT or Bcl10-deficient Treg cells into $Rag1^{-/-}$ recipient mice. In contrast to the WT Treg cells, the Bcl10-deficient Treg cells could not protect the recipient mice from weight loss and intestinal pathology (Fig. 4a, b). Furthermore, significant splenomegaly and mesenteric lymphadenopathy were observed in the mice treated with naive T cells transferred alone or with Bcl10-deficient Treg cells but not in those treated with naive T cells transferred with WT Treg cells. In line with this finding, the naive T cells transferred alone or with Bcl10-deficient Treg cells induced much higher numbers of $CD45.1^+$ IFNγ- and IL17A-producing cells in both the intestinal lamina propria and spleen of recipient mice than that naive T cells transferred with WT Treg cells (Fig. 4c, d).

Moreover, we performed an in vitro Treg-cell suppression assay by coculturing CFSE-labeled $CD45.1^+$ $CD4^+$ naive T cells alone or with WT (from $Bcl10^{+/+}Foxp3^{cre}$ mice) or Bcl10 KO (from $Bcl10^{fl/fl}Fxop3^{cre}$ mice) Treg cells in a specific ratio, and the results showed that the Bcl10-deficient Treg cells exhibited a defective inhibitory function (Fig. 4e, f). Together, these data suggest that Bcl10 is required for maintaining the suppressive function of Treg cells.

### Bcl10 maintains the identity and pupulation of Treg cells

Generally, Treg cells are responsible for maintaining immune homeostasis, and the phenotype observed in $Bcl10^{fl/fl}$ $Foxp3^{cre}$ mice indicated a profound loss of Treg-mediated homeostasis. Indeed, $Bcl10^{fl/fl}$ $Foxp3^{cre}$ mice showed a decreased percentage and absolute number of Treg cells in the spleen at 24 days old compared with $Bcl10^{+/+}$ $Foxp3^{cre}$ mice (Fig. 5a). In the peripheral lymph nodes, the Treg frequency but not the absolute number was decreased (Fig. 5a). Notably, the lymph nodes in $Bcl10^{fl/fl}$ $Foxp3^{cre}$ mice were significantly enlarged (Fig. 2c). These results suggested that Bcl10 played a role in the maintenance of the Treg-cell population. Moreover, the effector Treg (eTreg) cell population was largely decreased, and the central Treg (cTreg) cell population was significantly increased in $Bcl10^{fl/fl}$ $Foxp3^{cre}$ mice compared with littermate $Bcl10^{+/+}$ $Foxp3^{cre}$ mice (Fig. 5b). Although effector Tconv cell numbers were increased, naive Tconv cell numbers were decreased in $Bcl10^{fl/fl}$ $Foxp3^{cre}$ mice; these results were consistent with the data reported in Fig. 3a (Fig. 5b). These results indicate that Bcl10 is involved in controlling the conversion of cTregs into eTregs.

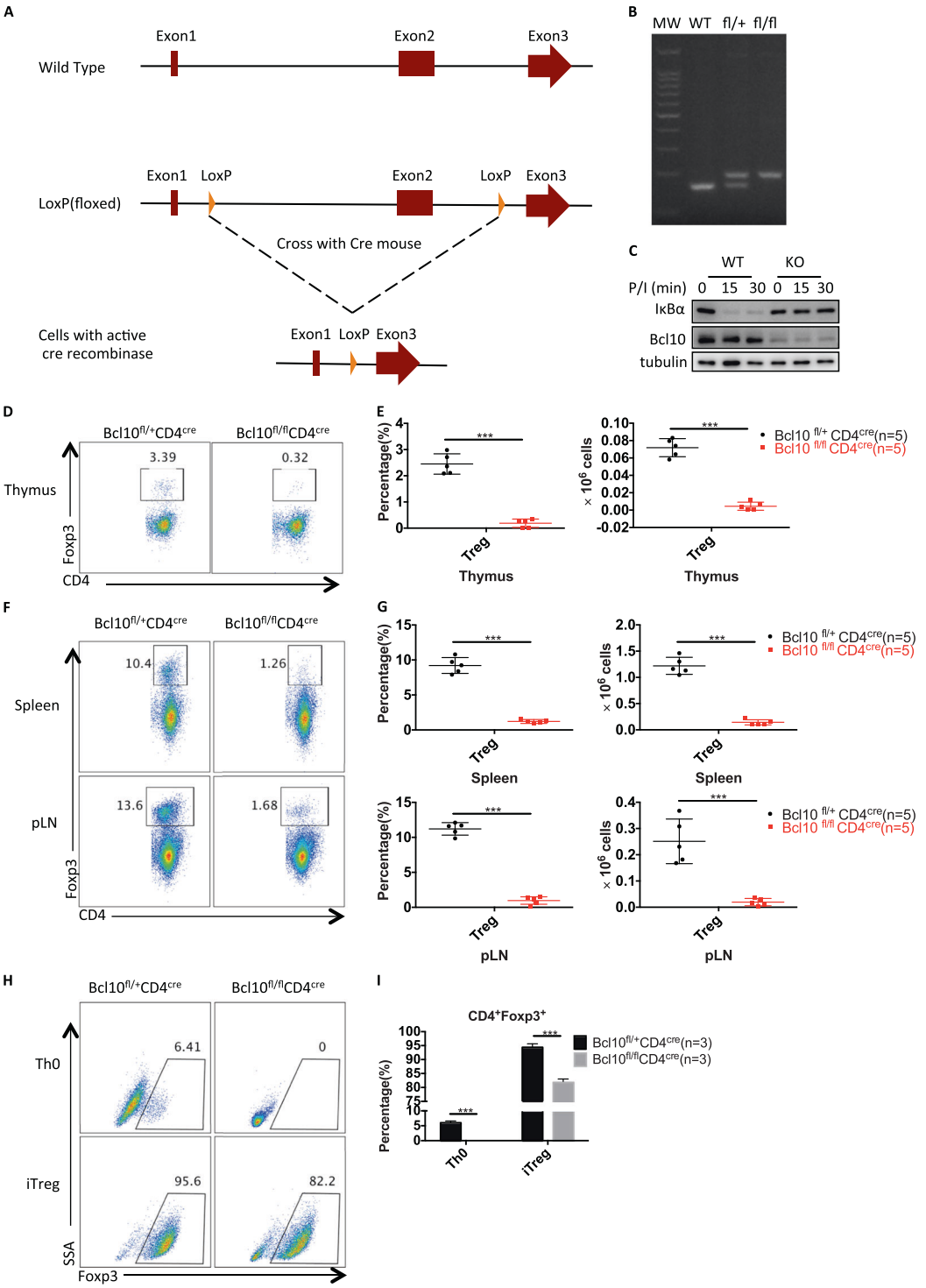


**Fig. 1** Bcl10 is required for the development of Treg cells. **a** The details are described in the methods and materials. A schematic graph of $Bcl10^{fl/fl}$ mouse generation is shown. Two loxP elements were inserted into introns 1 and 2. **b** Genotyping of WT ($Bcl10^{+/+}$), fl/+ ($Bcl10^{fl/+}$) and fl/fl ($Bcl10^{fl/fl}$) mice was performed by PCR. **c** WT (from $CD4^{cre}/Bcl10^{+/+}$ mice) and Bcl10-conditional KO (from $CD4^{cre}/Bcl10^{fl/fl}$ mice) pan T cells were stimulated with PMA (20 ng/mL) and ionomycin (200 ng/mL) for the indicated times, followed by immunoblotting analysis. **d**–**g** The thymus, spleen, and peripheral lymph nodes of 8- to 10-week-old $CD4^{cre}/Bcl10^{+/fl}$ and $CD4^{cre}/Bcl10^{fl/fl}$ mice were analyzed by FACS ($n = 5$ per group). **d** FACS plots show $CD4^+Foxp3^+$ cells gated on $CD4^+CD8^-$ cells in the thymus. **e** Statistical analyses were used to evaluate the $CD4^+Foxp3^+$ cell percentage (left) in the $CD4^+CD8^-$ cell population and absolute numbers (right) in the thymus. **f** FACS plots show $CD4^+Foxp3^+$ cells gated on $CD4^+CD8^-$ cells in the spleen or peripheral lymph nodes. **g** Statistical analyses were used to evaluate the $CD4^+Foxp3^+$ cell percentage (left) in the $CD4^+CD8^-$ cell population and absolute numbers (right) in the spleen or peripheral lymph nodes. **h**, **i** $CD4^+CD25^-CD44^-CD62L^+$ naive T cells sorted from a pooled spleen and lymph node suspensions from $Bcl10^{+/fl}CD4^{cre}$ or $Bcl10^{fl/fl}CD4^{cre}$ mice were stimulated by plate-bound anti-CD3/28 antibodies (5 μg/mL) alone (Th0) or in the presence of mouse IL-2 (10 μg/mL) and human TGF-β (2 ng/mL) (iTreg) for 3 days. Foxp3 induction in viable cells was detected in gated $CD4^+$ cells **h**, and a summary of the $Foxp3^+$ percentage is shown in **i**. Student's *t* test was used as the statistical test (*$p < 0.05$, **$p < 0.01$, and ***$p < 0.005$). All error bars represent SDs

Next, we found that IκBα degradation was blocked in Bcl10-deficient Treg cells (Fig. 5c), which showed a tendency similar to that in Tconv cells (Fig. 1c). This finding suggests that NF-κB activation, which plays a key role in the development of Treg cells and determines the size of the eTreg population, is inhibited in Bcl10-deficient Treg cells.[21,24] Moreover, the expression of KLRG1, an effector gene in Treg cells, was significantly decreased in Treg cells from $Bcl10^{fl/fl}Foxp3^{cre}$ mice compared with those from $Bcl10^{+/+}Foxp3^{cre}$ mice (Fig. 5d, e). Consistently, the mRNA level of *Klrg1* and that of another critical effector gene, *Icos*, were also significantly downregulated in Bcl10 KO Treg cells compared with WT Treg cells (Fig. 5f). We also found that some other Treg-associated suppressive genes, such as *Tgfb1*, *Il-10*, *Rel,* and *Irf4*, showed decreased expression in $Bcl10^{fl/fl}Foxp3^{cre}$ Treg cells (Fig. 5g). In addition, we observed loss of *Foxp3* and *Bcl10* mRNA expression in $Bcl10^{fl/fl}Foxp3^{cre}$ Treg cells on day 24 (Fig. 5g).

Considering that the eTreg population is critical in controlling autoreactive T cells, we conducted in vitro suppression assays by coculturing $CD45.1^+$ $CD4^+$ naive T cells with sorted eTregs and cTregs from $Bcl10^{+/+}Foxp3^{cre}$ (WT) or $Bcl10^{fl/fl}Foxp3^{cre}$ (KO) mice in a specific ratio. Although the eTreg cells displayed a better suppressive function than the cTregs, we found that Bcl10 was required for the suppressive function in both the eTregs and the cTregs (Fig. 6a). Furthermore, we isolated eTregs and cTregs from $Bcl10^{+/+}Foxp3^{cre}$ (WT) or $Bcl10^{fl/fl}Fxop3^{cre}$ (KO) mice and stimulated them with anti-CD3/CD28 antibodies and IL-2 for 48 h. Consistently, we observed that the Bcl10-deficient eTreg and cTreg cells exhibited defective expression of *Bcl10*, *Foxp3*, *Tgfb1*, *Klrg1,* and *Icos* but increased expression of *Ifng* (Fig. 6b). Together, these data indicate that Bcl10 is essential for the development and function of both eTregs and cTregs.

Interestingly, there was an increase in the frequency of effector $CD4^+$ T cells with a skewing toward IFNγ-secreting T helper 1 (Th1) cells in the spleen and LNs (Fig. 3c, g), and Bcl10-deficient Treg cells, which were derived from the spleen or peripheral lymph nodes of $Bcl10^{fl/fl}$ $Foxp3^{cre}$ mice, secreted much more IFNγ than Treg cells from $Bcl10^{+/+}Foxp3^{cre}$ mice (Fig. 6b, Fig. 7a, b). Given that ablation of NF-κB in Treg cells leads to increased expression of the inflammatory cytokine IFNγ[21] and that Bcl10 deficiency in Treg cells resulted in inactivation of NF-κB (Fig. 5c), the enhancement of IFNγ expression in Bcl10-deficient Treg cells may be partially owing to impaired NF-κB signaling. Moreover, Bcl10 loss in Treg cells led to a decrease in Nrp1 (Neuropilin-1) expression (Fig. 5g), and disruption of Nrp1 expression on Treg cells can increase the frequency of $IFNγ^+$ Treg cells,[36] indicating that Bcl10 in Treg cells may also partially regulate IFNγ expression in a Neuropilin-1-dependent manner. On the other hand, Foxp3 can directly repress IFNγ expression, and ChIP assay studies have detected Foxp3 bound to the *Spp1* locus, which encodes the type 1 cytokine osteopontin.[37,38] As Foxp3 expression was inhibited in Bcl10-deficient Treg cells (Fig. 5a, g), IFNγ expression was enhanced by the loss of Foxp3. Overall, the impact of Bcl10 on IFNγ expression is context dependent.

Similar to Th1 cells, Bcl10-deficient Treg cells displayed highly increased expression of the transcription factor T-bet (Fig. 7C, D). Accordingly, T-bet coordinates Th1 cell development and function by directly inducing the transcription of IFNγ and other related genes.[39,40] Moreover, T-bet is expressed in Treg cells and drives IFNγ expression, which is required for the function of Treg cells.[41,42] In addition, it has been reported that HIF-1α induces IFNγ production by directly binding to the IFNγ promoter in macrophages[43] and HIF-1α also directly binds to the IFNγ promoter in VHL-deficient Treg cells, which have increased IFNγ production and an impaired suppressive function.[44] In addition, VHL-deficient Treg cells also show increased T-bet and T-bet-driven IFNγ expression.[44] We also found that HIF-1α was expressed at higher levels in Bcl10-deficient Treg cells than in WT Treg cells (Figs. 7C and 6D). Moreover, Bcl10 deficiency led to large increases in $IFNγ^+$T-bet$^+$ and $IFNγ^+$HIF-1α$^+$ Treg-cell pupulations (Fig. 7e, f). In addition, we treated WT and KO Treg cells with the HIF-1α inhibitor PX-478 combined with stimulation with anti-CD3/anti-CD28 antibodies, and the results showed that HIF-1α expression was slightly downregulated after PX-478 treatment and that IFNγ production was partially reduced (supplementary Fig. 1A and 1B). Thus, Bcl10-deficient Treg cells convert from a suppressive immunoregulatory cell type into an IFNγ-secreting pathogenic cell type in $Bcl10^{fl/fl}$ $Foxp3^{cre}$ mice, which may be dependent on the expression of the transcription factors T-bet and HIF-1α.

## DISCUSSION

Conventional and Treg cells play completely opposite roles in regulating the adaptive immune response even though they develop from the same progenitors and share many similar receptors and signaling transduction pathways. Bcl10 regulates the development and function of Tconv cells by mediating NF-κB activation through forming the CBM signalosome after the activation of TCR signaling. In this study, we specifically deleted Bcl10 in $CD4^+$ T cells or Treg cells and found that Bcl10 was required for the development and suppressive function of Treg cells. $Bcl10^{fl/fl}Foxp3^{cre}$ mice, in which Bcl10 is specifically deficient in Treg cells, showed severe lethal autoimmune diseases. Tconv cells are unregulated and overactivated in the absence of functional Treg cells. In contrast, unlike $Bcl10^{fl/fl}Foxp3^{cre}$ mice, $Bcl10^{fl/fl}CD4^{cre}$ mice, in which Bcl10 is deficient in all T cells, did not display autoimmune diseases. Conditionally deleting Bcl10 in Treg cells led to severe spontaneous autoimmune diseases owing to the impaired function of the Treg cells, resulting in immune disorders, whereas systemically deleting Bcl10 in all T cells did not induce an autoimmune reaction. This is because Bcl10 acts downstream of TCR signaling in both Tconv and Treg cells to control their development and activation.

Bcl10-deficient Treg cells exhibited highly impaired immunosuppressive function in an in vivo T-cell transfer-induced colitis model and in vitro Treg suppression assay. Mechanistically, the Treg cells in $Bcl10^{fl/fl}Foxp3^{cre}$ mice showed less expression of effector and suppressive genes, including *Icos*, *Klrg1, Tgfb1, Il-10*, and *IRF4*, a decreased population of highly suppressive functional eTregs, and conversion from a suppressive cell type to a proinflammatory cell type with high expression of the inflammatory factor IFNγ. Moreover, Bcl10-deficient Treg cells were impaired in NF-κB activation and Foxp3 and Nrp1 expression, which all contributed to the dysfunction of the Bcl10-deficient Treg cells.

During the time of our current study, several studies[45–47] reported the phenotype of specific deficiencies in the CBM complex in Treg cells. They found elevated expression of IFNγ in Carma1-deficient Treg cells from $Carma^{fl/fl}$ $Foxp3^{cre}$ mice, which was only partially dependent on the transcription factor T-bet.[46] Consistently, we also found increased expression of IFNγ and T-bet in Bcl10-deficient Treg cells. Furthermore, we also observed elevated expression of HIF-1α in Bcl10-deficient Treg cells. As VHL-deficient Treg cells convert into Th1-like effector T cells with high IFNγ expression directly regulated by the transcription factor hypoxia-inducible factor 1α (HIF-1α),[44] it is possible that the conversion of Carma1-deficient Treg cells into IFNγ-producing cells may also be partially dependent on HIF-1α activation. Even though the impact of T-bet on IFNγ expression in Treg cells has been documented and shown to be required for Treg-cell functioning.[41,42] many studies have also shown that IFNγ production by Treg cells induces Th1 responses and tissue damage.[44,46,48–50]

The phenotype of Bcl10-deficient mice was confirmed by identifying human primary immune deficiencies, indicating that the function of Bcl10 is highly conserved between mice and humans.[51] In inflammation or malignancy induced by abnormal

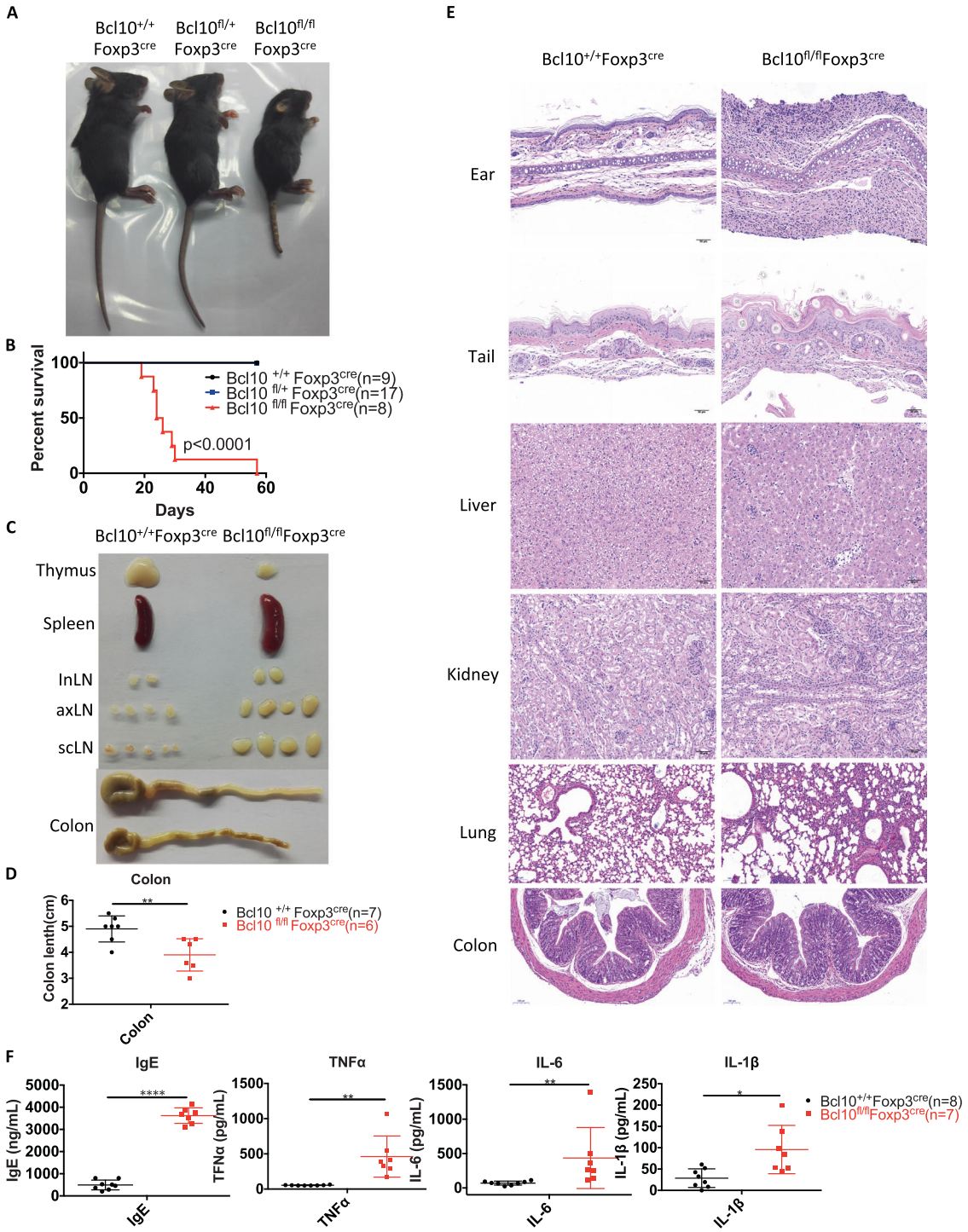


**Fig. 2** Bcl10 deficiency in Treg cells leads to lethal autoimmune inflammation. **a** Image of 24-day-old littermate female mice with different genotypes: Bcl10$^{+/+}$Foxp3$^{cre}$, Bcl10$^{fl/+}$Foxp3$^{cre}$, or Bcl10$^{fl/fl}$Foxp3$^{cre}$. **b** Survival of Bcl10$^{+/+}$Foxp3$^{cre}$, Bcl10$^{fl/+}$Foxp3$^{cre}$, and Bcl10$^{fl/fl}$Foxp3$^{cre}$ mice ($n = 9$, 17, and 8 per group, respectively). **c** Images of the thymus, spleen, inLN (inguinal lymph node), axLN (axillary lymph node), scLN (superficial neck lymph node), and colon harvested from 24-day-old female littermate mice with different genotypes: Bcl10$^{+/+}$Foxp3$^{cre}$, or Bcl10$^{fl/fl}$Foxp3$^{cre}$. **d** Colon length in 24-day-old Bcl10$^{+/+}$Foxp3$^{cre}$, and Bcl10$^{fl/fl}$Foxp3$^{cre}$ mice ($n = 7$ or 6 per group). **e** H&E staining of the skin of the ear and tail and tissue samples from the liver, kidney, lung, and colon from 24-day-old mice with different genotypes: Bcl10$^{+/+}$Foxp3$^{cre}$, or Bcl10$^{fl/fl}$Foxp3$^{cre}$. **f** Enzyme-linked immunosorbent assay (ELISA) analysis of IgE, TNFα, IL-6, and IL-1β levels in serum samples obtained from Bcl10$^{+/+}$Foxp3$^{cre}$ ($n = 8$) or Bcl10$^{fl/fl}$Foxp3$^{cre}$ ($n = 7$) mice on day 24. Student's *t* test was used as the statistical test (*$p < 0.05$, **$p < 0.01$, and ***$p < 0.005$). All error bars represent SDs

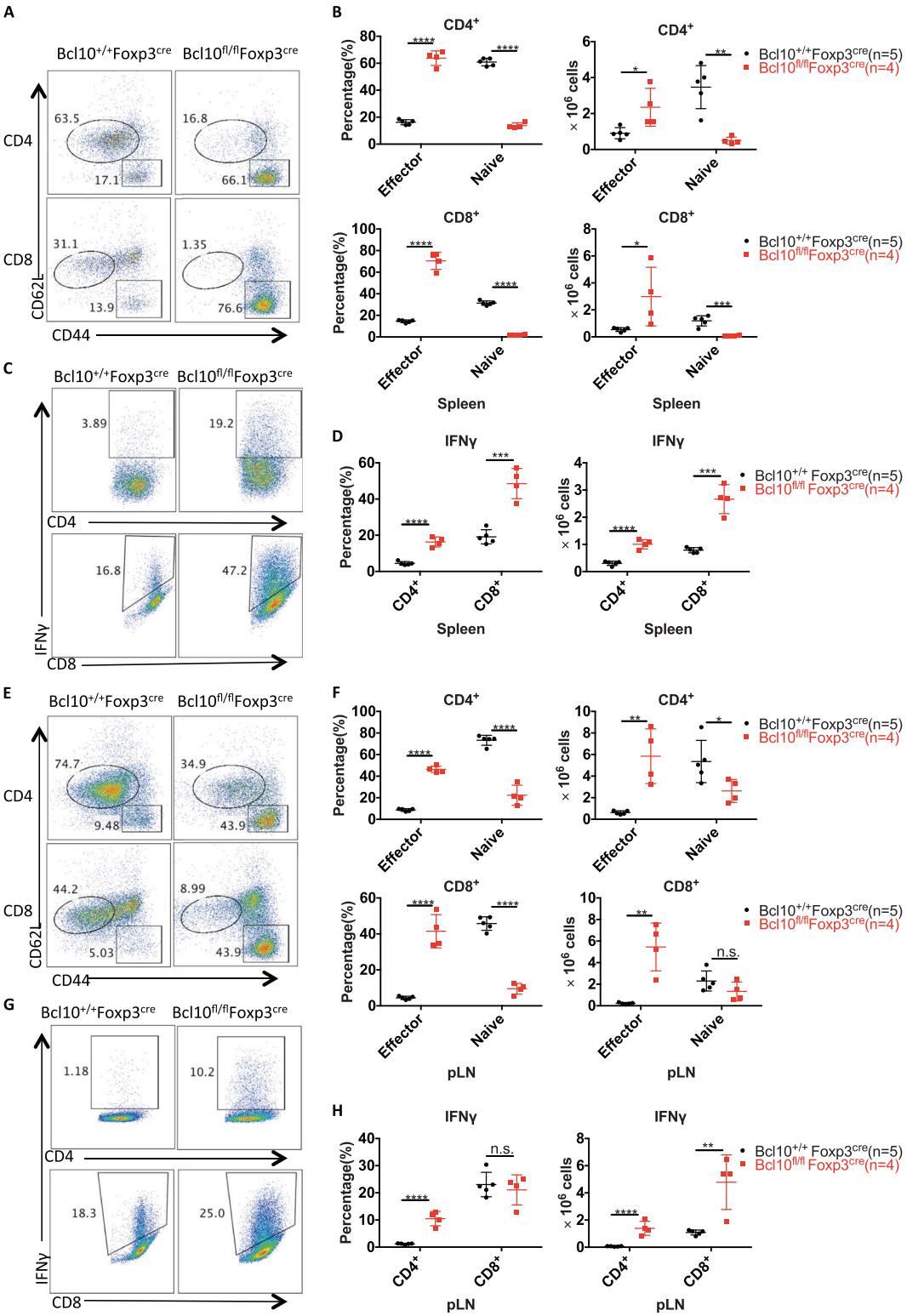


**Fig. 3** Bcl10 deficiency in Treg cells results in overactivation of T cells. Spleens and peripheral lymph nodes from 24-day-old $Bcl10^{+/+}Foxp3^{cre}$ or $Bcl10^{fl/fl}Foxp3^{cre}$ mice were analyzed by FACS ($n = 5$ or 4 per group). **a** Representative CD44 and CD62L expression in splenic $CD4^+$ and $CD8^+$ T cells. **b** Percentages (left) and absolute numbers (right) of naive ($CD44^{lo}CD62L^{hi}$) and effector ($CD44^{hi}CD62L^{lo}$) splenic $CD4^+$ or $CD8^+$ T cells. **c** Representative data for IFNγ-producing $CD4^+$ or $CD8^+$ T cells in the spleen after ex vivo stimulation with PMA (50 ng/mL) and ionomycin (500 ng/mL) for 4 h. **d** Percentages (left) and absolute numbers (right) of IFNγ-producing $CD4^+$ or $CD8^+$ T cells in the spleen after ex vivo stimulation with PMA (50 ng/mL) and ionomycin (500 ng/mL) for 4 h. **e** Representative CD44 and CD62L expression in $CD4^+$ and $CD8^+$ T cells from the peripheral lymph nodes. **f** Percentages (left) and absolute numbers (right) of naive ($CD44^{lo}CD62L^{hi}$) and effector ($CD44^{hi}CD62L^{lo}$) peripheral lymph node $CD4^+$ or $CD8^+$ T cells. **g** Representative data for IFNγ-producing $CD4^+$ or $CD8^+$ T cells in the peripheral lymph nodes. **h** Percentages (left) and absolute numbers (right) of IFNγ-producing $CD4^+$ or $CD8^+$ T cells in the peripheral lymph nodes. Student's *t* test was used as the statistical test (n.s. = no significance, $*p < 0.05$, $**p < 0.01$, and $***p < 0.005$). All error bars represent SDs

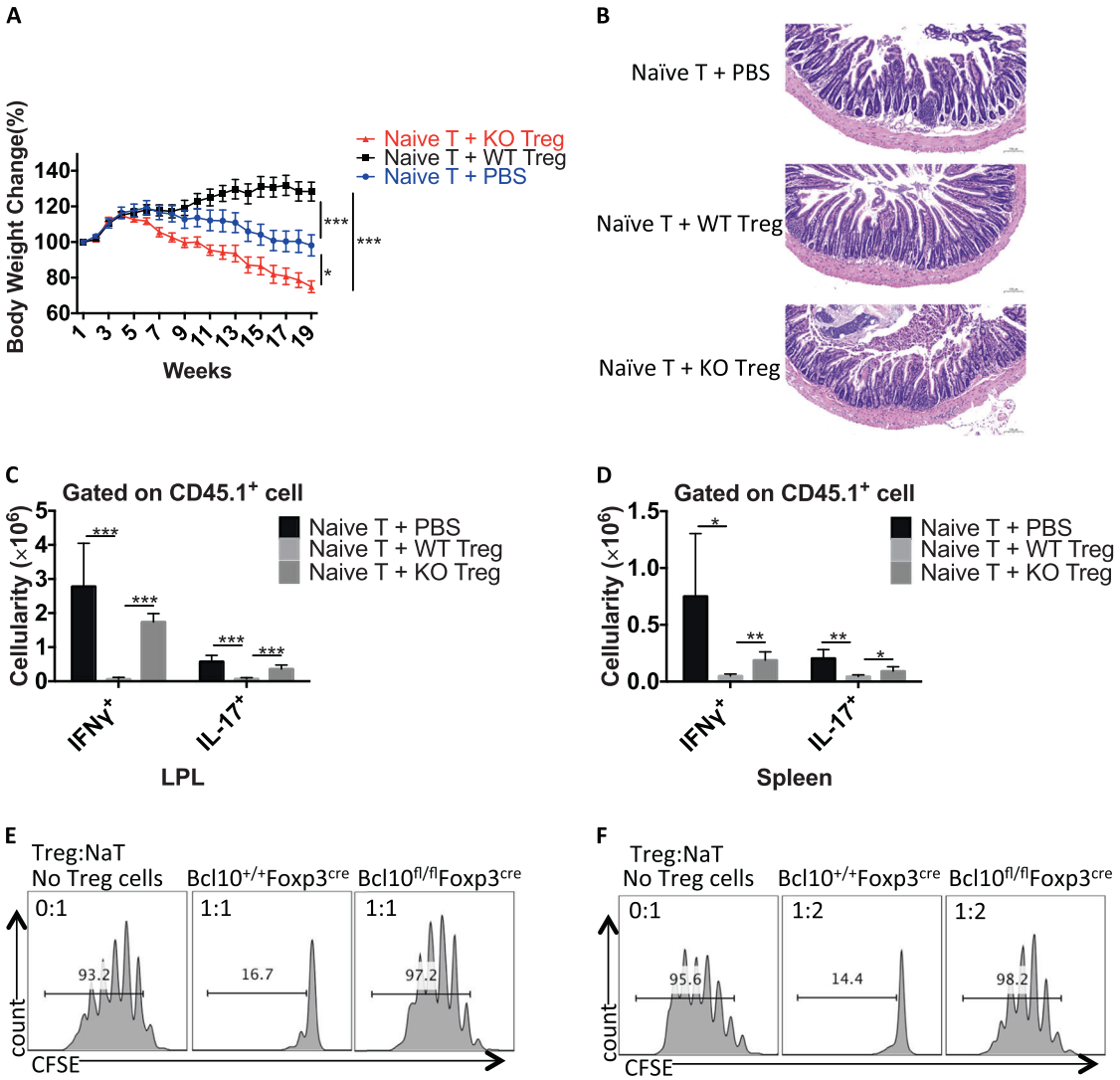


**Fig. 4** Bcl10 is required for the suppressive function of Treg cells. $CD45.1^+CD4^+CD25^-CD44^-CD62L^+$ naive T cells were isolated from the spleen and lymph nodes of $CD45.1^+$ mice, and $CD45.2^+CD4^+YFP^+$ Treg cells were isolated from $Bcl10^{+/+}Foxp3^{cre}$ (WT) or $Bcl10^{fl/fl}Foxp3^{cre}$ (KO) mice. Naive T cells alone (Naive T + PBS) or with WT Treg (Naive T + WT Treg) or KO Treg (Naive T + KO Treg) cells were intravenously injected into $Rag1^{-/-}$ recipient mice. **a** Body weight changes in $Rag1^{-/-}$ recipient mice receiving different combinations of T cells in the T cell transfer-induced colitis model. **b** H & E staining of the small intestine of $Rag1^{-/-}$ recipient mice at 18 weeks after receiving different combinations of T cells. **c** Absolute numbers of IFNγ- and IL17A-producing $CD45.1^+$ T cells in the lamina propria of the large intestine (LPL) after ex vivo stimulation with PMA (50 ng/mL) and ionomycin (500 ng/mL) for 4 h. **d** Absolute numbers of IFNγ- and IL17A-producing $CD45.1^+$ T cells in the spleen after ex vivo stimulation with PMA (50 ng/mL) and ionomycin (500 ng/mL) for 4 h. **e** and **f** In vitro Treg-cell suppression assay: CFSE-labeled naive $CD4^+$ T cells (from $CD45.1^+$ mice) cultured alone or cocultured with WT (from $Bcl10^{+/+}Foxp3^{cre}$ mice) or KO (from $Bcl10^{fl/fl}Foxp3^{cre}$ mice) Treg cells at a 1:1 **e** or 2:1 **f** ratio in the presence of irradiated splenocytes and an anti-CD3 antibody. Student's *t* test was used as the statistical test (*$p < 0.05$, **$p < 0.01$, and ***$p < 0.005$). All error bars represent SDs

expression of Bcl10, inhibiting Bcl10-related signaling can relieve the inflammatory reaction in diseases such as psoriasis and colitis. Our finding that specifically disrupting Bcl10 signaling in Treg cells leads to the inhibition of Treg functions may be a therapeutic approach for cancer immunotherapy. For example, Treg cells suppress antitumor immunity, and it is reported that the tumor environment demonstrates increased Treg-cell numbers in tumor samples treated with an infusion of EGFRvIII CAR-T cells compared with tumor specimens without CAR-T-cell infusion. However, it is not clear where these Treg cells are derived from.[52] However, directly eliminating Treg cells does not enhance the immunotherapy effect because apoptotic Treg cells mediate superior immunosuppression.[53] Therefore, deleting Bcl10 in Treg cells may be a good approach to enhance the function of CAR-T cells for tumor immunotherapy.

## MATERIALS AND METHODS

### Mice

All mice were housed in isolated ventilated cages (maximum of six mice per cage) in a barrier facility at Tsinghua University. The mice were maintained on a 12/12-hour light/dark cycle at 22–26°C with sterile pellet food and water provided ad libitum. The laboratory animal facility was accredited by the AAALAC (Association for Assessment and Accreditation of Laboratory Animal Care International), and the IACUC (Institutional Animal Care and Use Committee)

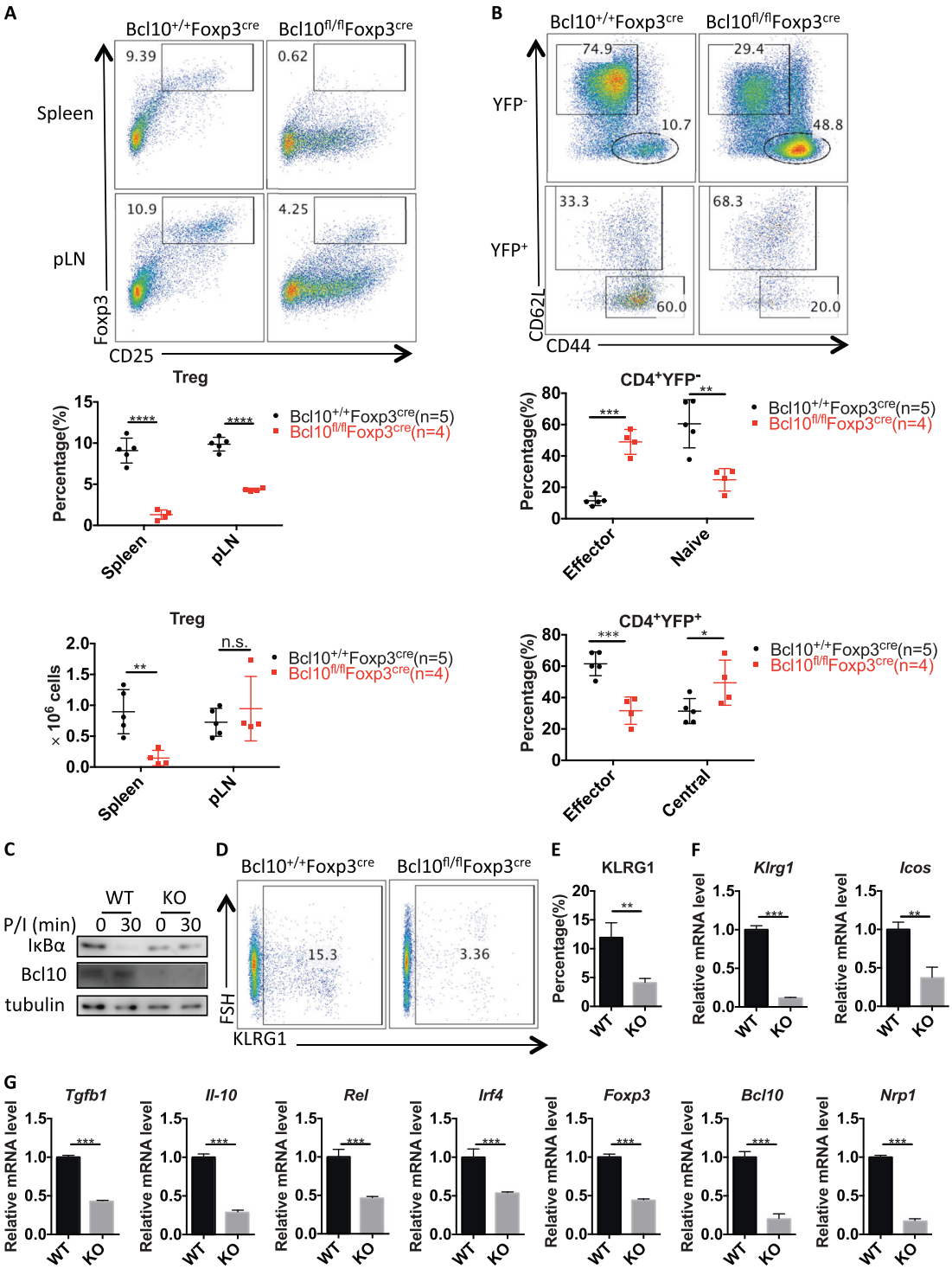


**Fig. 5** Bcl10 is essential for maintaining the identity and population of Treg cells. Spleens and peripheral lymph nodes from 24-day-old Bcl10$^{+/+}$Foxp3$^{cre}$ or Bcl10$^{fl/fl}$Foxp3$^{cre}$ mice were analyzed by FACS ($n = 5$, 4, or 3 per group). **a** FACS plots represent CD4$^+$CD25$^+$Foxp3$^+$ (Treg) cells gated on the CD4$^+$CD8$^-$ cells in the spleen or peripheral lymph nodes (above). Statistical analyses were used to evaluate the CD4$^+$CD25$^+$Foxp3$^+$ cell percentage in the CD4$^+$CD8$^-$ cell population and the absolute numbers in the spleen or peripheral lymph nodes (below). **b** FACS plots represent effector (CD44$^{hi}$CD62L$^{lo}$) and naive or central (CD44$^{lo}$CD62L$^{hi}$) cells gated on CD4$^+$YFP$^-$(Foxp3$^-$) (above) or CD4$^+$YFP$^+$(Foxp3$^+$) (below) cells in the spleen and lymph nodes (above). Statistical analyses were used to evaluate the effector (CD44$^{hi}$CD62L$^{lo}$) and naive or central (CD44$^{lo}$CD62L$^{hi}$) cell percentages in the CD4$^+$YFP$^-$(Foxp3$^-$) (above) and CD4$^+$YFP$^+$(Foxp3$^+$) (below) cell populations in the spleen and lymph nodes. **c** WT (from Bcl10$^{+/+}$Foxp3$^{cre}$ mice) and Bcl10 KO (from Bcl10$^{fl/fl}$Foxp$^{cre}$ mice) Treg cells were stimulated with PMA (20 ng/mL) and ionomycin (200 ng/mL) for the indicated time, followed by immunoblotting analysis. **d** FACS plots represent KLRG$^+$ cells gated on the CD4$^+$YFP$^+$ cells in the spleen and lymph nodes. **e** The percentage of KLRG$^+$ cells gated on the CD4$^+$YFP$^+$ cells in the spleen and lymph nodes (WT: Bcl10$^{+/+}$Foxp3$^{cre}$ mice ($n = 4$), KO: Bcl10$^{fl/fl}$Foxp3cre mice ($n = 3$)) is shown. **f** and **g** The mRNA levels of Klrg1, Icos **f**, Tgfb1, Il-10, Rel, Irf4, Nrp1, Foxp3, and Bcl10 **g** were measured by qRT-PCR in WT (from Bcl10$^{+/+}$Foxp3$^{cre}$ mice) and KO (from Bcl10$^{fl/fl}$Foxp3cre mice) Treg cells (CD4$^+$YFP$^+$ cells) (mean ± SEM, $n = 3$). Student's $t$ test was used as the statistical test (n.s. = no significance, *$p < 0.05$, **$p < 0.01$, and ***$p < 0.005$). All error bars represent SDs

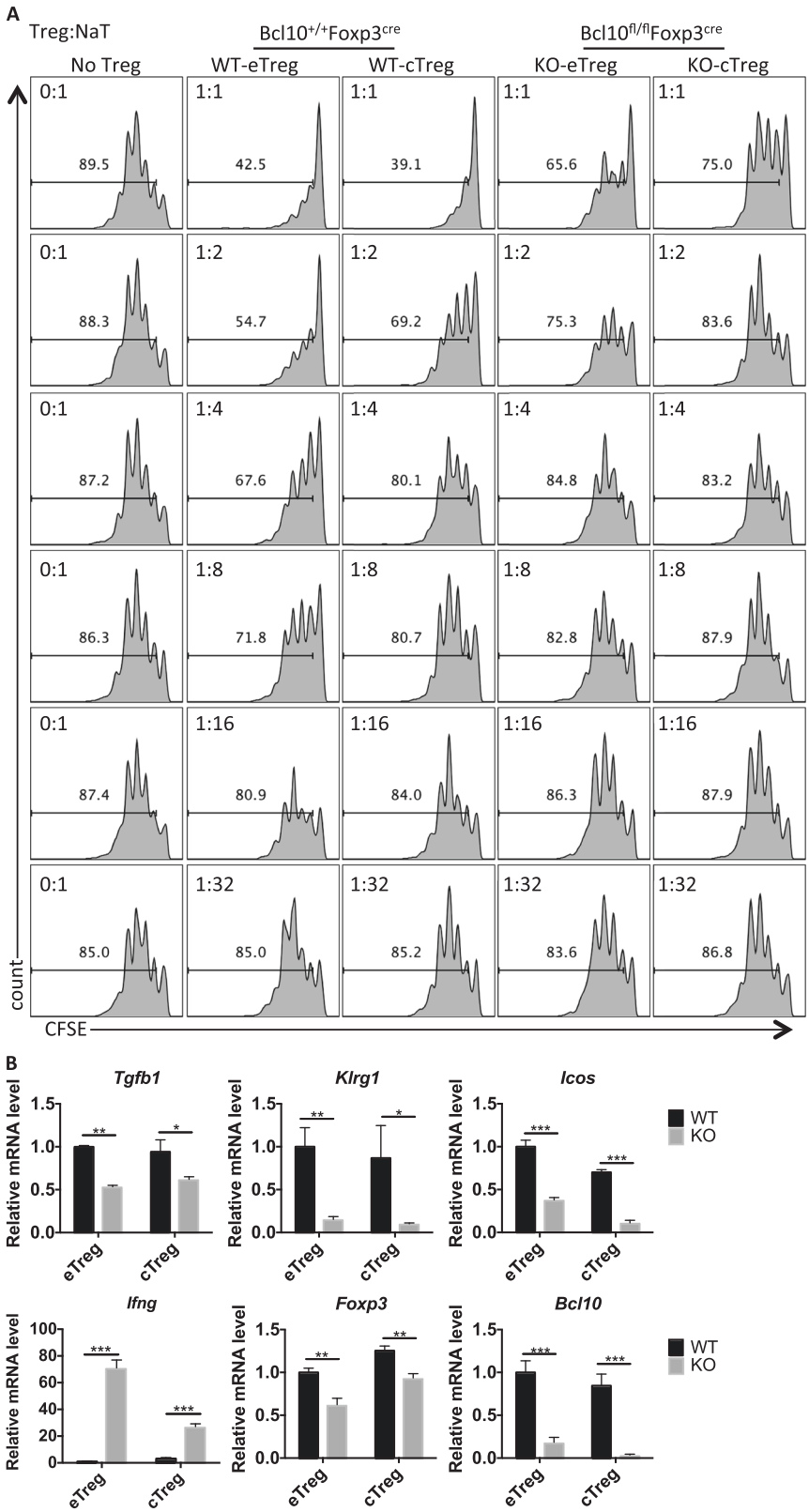


**Fig. 6** Bcl10 functions in both eTreg cells and cTreg cells. **a** In vitro suppression assay for eTreg and cTreg cells: CFSE-labeled $CD4^+$ naive T cells (from $CD45.1^+$ mice) cultured alone or cocultured with WT-eTreg, WT-cTreg (from $Bcl10^{+/+}Foxp3^{cre}$ mice), KO-eTreg, or KO-cTreg (from $Bcl10^{fl/fl}Foxp3^{cre}$ mice) cells at the indicated ratio in the presence of irradiated splenocytes and an anti-CD3 antibody. **b** The mRNA levels of Tgfb1, Klrg1, Icos, Ifng, Foxp3, and Bcl10 were determined by qRT-PCR in WT (from $Bcl10^{+/+}Foxp3^{cre}$ mice) and KO (from $Bcl10^{fl/fl}$Foxp3cre mice) eTreg or cTreg cells (mean ± SEM, $n = 3$). Student's $t$ test was used as the statistical test (*$p < 0.05$, **$p < 0.01$, and ***$p < 0.005$). All error bars represent SDs

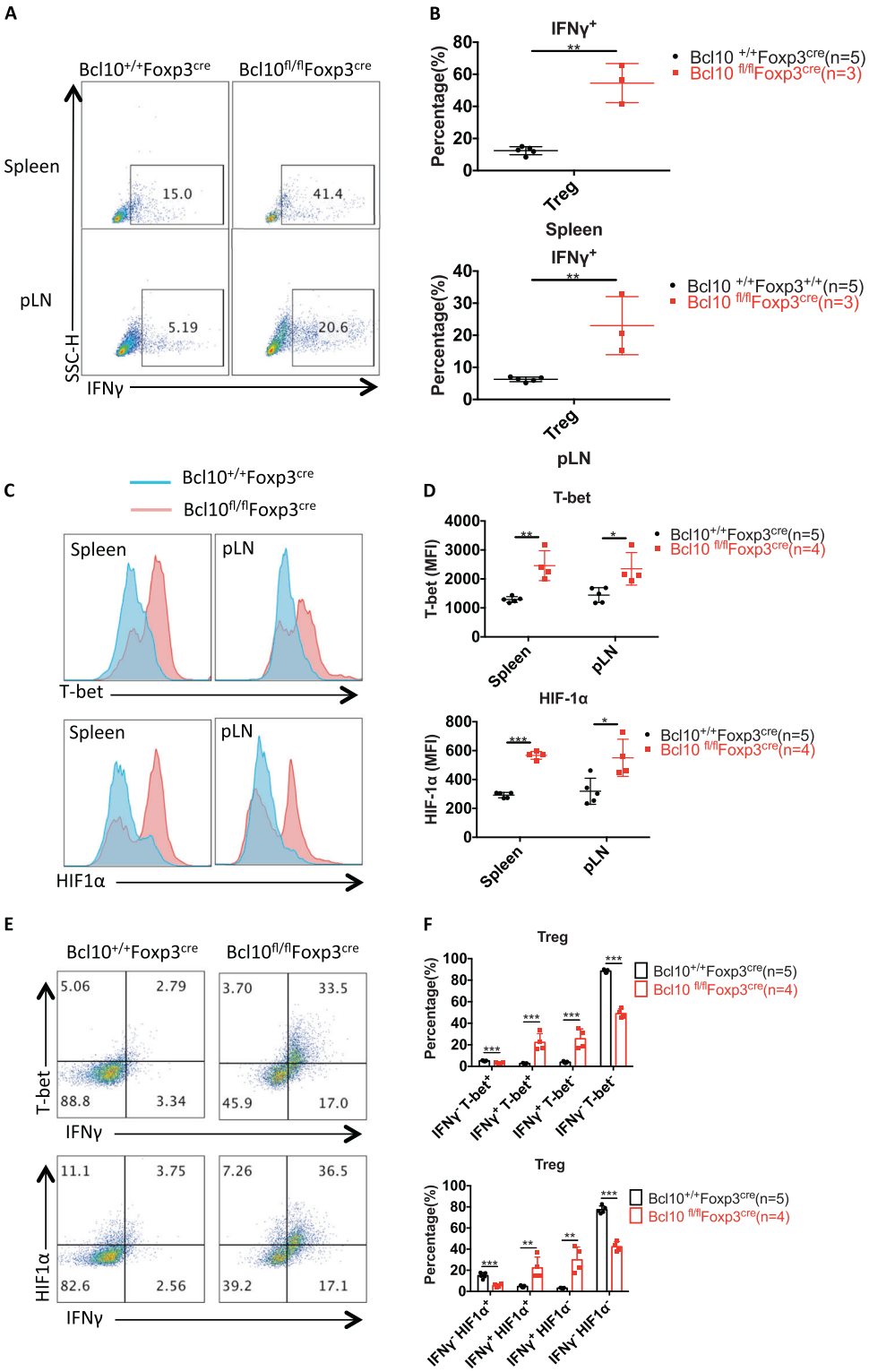


**Fig. 7** Bcl10-deficient Treg cells convert into proinflammatory cells. Spleens and peripheral lymph nodes from 24-day-old Bcl10$^{+/+}$Foxp3$^{cre}$ or Bcl10$^{fl/fl}$Foxp3$^{cre}$ mice were analyzed by FACS ($n = 5$, 4, or 3 per group). **a** Representative data for IFNγ-producing CD4$^{+}$Foxp3$^{+}$IFNγ$^{+}$ Treg cells gated on CD4$^{+}$Foxp3$^{+}$ Treg cells in the spleen or peripheral lymph nodes after ex vivo stimulation with PMA (50 ng/mL) and ionomycin (500 ng/mL) for 4 h. **b** Percentages of IFNγ-producing CD4$^{+}$ Foxp3$^{+}$ Treg cells of the total CD4$^{+}$Foxp3$^{+}$ Treg cells in the spleen (above) or peripheral lymph nodes (below) after ex vivo stimulation with PMA (50 ng/mL) and ionomycin (500 ng/mL) for 4 h. **c** and **d** T-bet and HIF-1α expression in Treg cells (CD4$^{+}$Foxp3$^{+}$) in the spleen and peripheral lymph nodes of Bcl10$^{+/+}$Foxp3$^{cre}$ or Bcl10$^{fl/fl}$Foxp3$^{cre}$ mice. The MFI (mean fluorescence intensity) was measured by flow cytometry in **c**, the values were calculated, and a combined plot for **c** is shown in **d**. **e** FACS plots representing the expression levels of IFNγ and T-bet (above) or HIF-1α (below) in gated CD4$^{+}$Foxp3$^{+}$ Treg cells from the spleen and lymph nodes. **f** Statistical analysis of the expression levels of IFNγ and T-bet (above) or the HIF-1α-positive (below) cell percentage in CD4$^{+}$Foxp3$^{+}$ Treg cells from the spleen and lymph nodes. Student's *t* test was used as the statistical test (*$p < 0.05$, **$p < 0.01$, and ***$p < 0.005$). All error bars represent SDs

of Tsinghua University approved all animal protocols used in this study. $CD4^{cre}$, $Foxp3^{cre\text{-}YFP}$, and $Rag1^{-/-}$ mice were kindly provided by Professor Chen Dong at Tsinghua University. $CD45.1^{+}$ mice were kindly provided by Professor Li Wu at Tsinghua University.

### Generation of $Bcl10^{fl/fl}$ mice

$Bcl10^{fl/fl}$ mice were generated on a C57BL/6 background with CRISPR/Cas9 technology. The single-guide RNA (sgRNA) targeting sequence (Supplemental Table I) was designed by using an online tool (http://crispr.mit.edu/) and was synthesized with a *Streptococcus pyogenes* Cas9-guide RNA efficiency of target detection kit (Viewsolid Biotech). Then, the sgRNA and Cas9 mRNA were transcribed in vitro with the MEGAshortscript T7 Transcription Kit and mMESSAGE mMACHINE T7 ULTRA Transcription Kit (Life Technologies) according to the manufacturer's protocol. Both the sgRNA and the Cas9 mRNA were purified with the MEGAclear Kit (Life Technologies) and dissolved in RNase-free water. Donor DNA, which comprised single-strand oligos containing a loxP sequence, was synthesized at Sangon Biotech (Shanghai, China). Finally, 20 μl of mixture containing the sgRNA (20 ng/ml), Cas9 mRNA (40 ng/ml), and donor oligos (60 ng/ml) was injected into zygotes. The microinjection was accomplished at the Laboratory Animal Research Center, Tsinghua University. The founder mice were genotyped with manually designed specific primers (Supplemental Table I) and confirmed by TA cloning (TransGen Biotech) and sequencing.

### Flow cytometry and cell sorting

The relevant protocol and antibody information have been described previously.[47]

### In vitro Treg-cell differentiation

$CD4^{+}$ T cells were enriched with Miltenyi CD4 (L3T4) microbeads from single-cell suspensions of spleens and lymph nodes from $Bcl10^{+/+}CD4^{cre}$ or $Bcl10^{fl/fl}$ $CD4^{cre}$ mice, and then $CD4^{+}CD25^{-}CD44^{-}CD62L^{+}$ naive T cells were sorted by flow cytometry (BD FACSAriaII). The naive T cells were cultured in complete Roswell Park Memorial Institute 1640 medium (Life Technologies) and stimulated with 5 μg/mL plate-coated anti-CD3/CD28 antibodies alone (Th0 conditions) or in the presence of mouse IL-2 (10 μg/mL) and human TGF-β (2 ng/mL) (Treg conditions). Forty-eight hours later, 0.5 mL of fresh medium was added if needed. After 72 h, the cells were collected and stained for fluorescence-activated cell sorting (FACS) analysis.

### In vitro Treg suppression assay

CFSE-labeled $CD45.1^{+}$ $CD4^{+}$ naive T cells ($4 \times 10^5$ cells/mL, 50 μL) alone or cocultured with Treg cells (50 μL) at different ratios in the presence of $2 \times 10^6$ cells/mL (50 μL) irradiated (30 gray) splenocytes as APCs and medium containing 4 μg/ml anti-CD3 antibody (50 μL) in a 96-well U-bottom plate. Three days later, CFSE dilution was detected, which indicated the Treg-cell suppression ability.

### Immunoblot analysis

T cells were lysed in an NP-40 lysis buffer containing 50 mM HEPES (pH 7.4), 150 mM NaCl, 1% Nonidet P-40, 1 mM EDTA, 1 mM $Na_3VO_4$, 1 mM NaF, 1 mM PMSF, and a protease inhibitor mixture (Roche Diagnostics, 4693116001). The cell lysates were subjected to sodium dodecyl sulphate polyacrylamide gel electrophoresis (SDS–PAGE) and western blot analysis. The samples were boiled and separated on a 10% SDS–PAGE gel and transferred to nitrocellulose membranes. The immunoblots were incubated with specific primary antibodies, followed by incubation with HRP-conjugated secondary antibodies. Then, they were developed by the enhanced chemiluminescence method according to the manufacturer's protocol (Merck Millipore, WBKLS0500).

### Enzyme-linked immunosorbent assay

Immunoglobulins against autoantigens in mouse serum samples were measured with ELISA kits (eBioscience) according to the manufacturer's instructions.

### Tissue histology

Skin from the ears or tail and tissue samples from the lungs, liver, kidneys, and colon of $Bcl10^{+/+}Foxp3^{cre}$ or $Bcl10^{fl/fl}Foxp3^{cre}$ mice were dissected, fixed in a 4% paraformaldehyde tissue fixation buffer (Solarbio, P1110-500) for 24 h, and stained with H&E at Wuhan Google Biotechnology Co., Ltd.

### T cell transfer-induced colitis model

$CD45.1^{+}CD4^{+}CD25^{-}CD44^{-}CD62L^{+}$ naive T cells were sorted according to the protocol used for in vitro differentiation of Treg cells from cells from $CD45.1^{+}$ mice. $CD45.2^{+}$ $CD4^{+}CD25^{+}YFP^{+}$ Treg cells were sorted from $Bcl10^{+/+}Foxp3^{cre}$ or $Bcl10^{fl/fl}Foxp3^{cre}$ mice. In total, $5 \times 10^5$ naive T cells alone or with $1 \times 10^5$ WT or Bcl10 KO Treg cells were intravenously injected into recipient $Rag1^{-/-}$ mice. Weight changes were monitored weekly, and the intestine and spleen were collected for H&E staining and FACS analysis.

### Real-time quantitative PCR (qPCR)

Snap-frozen mouse tissue samples or cells were dissolved directly in TRIzol (Invitrogen, 15596018). Total RNA was extracted, and reverse transcription was performed with the RevertAid First Strand cDNA Synthesis Kit (Thermo Scientific). An ABI 7500 Real-Time PCR system (Applied Biosystems) and Power SYBR Green PCR Master Mix (Genestar) were used for qPCR. The results were normalized to those for GAPDH, and quantification was performed with the 2-ΔΔCt method. The following primers were used for PCR:

Irf4, 5′-TCCTCTGGATGGCTCCAGATG-3′ (forward) and 5′-CACCA AAGCACAGAGTCACCT-3′ (reverse);

Il-10, 5′-ATAACTGCACCCACTTCCCAGTC-3′ (forward) and 5′-CCCAAGTAACCCTTAAAGTCCTGC-3′ (reverse);

Tgfb1, 5′-CCACCTGCAAGACCATCGAC-3′ (forward) and 5′-CTGGCGAGCCTTAGTTTGGAC-3′ (reverse);

Ifng, 5′-GCCACGGCACAGTCATTGA-3′ (forward) and 5′-TGCTGATGGCCTGATTGTCTT-3′ (reverse);

Klrg1, 5′-GGACGAGGAATGGTAGCCAC-3′ (forward) and 5′-GTAAGGAGATGGTAGCCAC-3′ (reverse);

Rel, 5′-CAACTGGAGAAGGAAGATTCA-3′ (forward) and 5′-TGGAACTCCTGAAGACCTG-3′ (reverse);

Nrp1, 5′-ACCTCACATCTCCCGGTTACC-3′ (forward) and 5′-AAGGTGCAATCTTCCCACAGA-3′ (reverse);

Icos, 5′-ATGAAGCCGTACTTCTGCCG-3′ (forward) and 5′-CGCATTTTTAACTGCTGGACAG-3′ (reverse);

Bcl10, 5′-TCCCTCACGGAGGAGGATTTG-3′ (forward) and 5′-ACTTCCCAGCCCGTTTTCTAC-3′ (reverse);

Foxp3, 5′- CACCTATGCCACCCTTATCCG-3′ (forward) and 5′-CATGCGAGTAAACCAATGGTAGA-3′ (reverse); and

GAPDH, 5′-AACAGCAACTCCCACTCTTC-3′ (forward) and 5′-CCTGTTGCTGTAGCCGTATT-3′ (reverse).

### Statistical analyses

Age- and sex-matched mice were randomly assigned for experiments. The animal numbers used for all experiments are outlined in the corresponding figure legends. No animals were excluded from statistical analyses, and the investigators were not blinded in the studies. No statistical methods were used to predetermine sample sizes. All studies were performed at least three times independently. The results are reported as the mean ± s.e.m. Comparisons of different groups were carried out using a two-tailed unpaired Student's *t* test or one-way analysis of variance. Differences were considered statistically significant at $P < 0.05$.

Compliance with ethics guidelines
All institutional and national guidelines for the care and use of laboratory animals were followed. The authors declare that they have no conflicts of interest.

## ACKNOWLEDGEMENTS

We thank Dr. Chen Dong for providing the Rag1$^{-/-}$, CD4$^{cre}$ and Foxp3$^{cre\text{-}YFP}$ mice and Dr. Li Wu for providing the CD45.1$^{+}$ mice. We thank the Laboratory Animal Research Center of Tsinghua University for help with microinjections. This work was supported by grants from the National Natural Science Foundation of China (81570211 to X.L. and 31670904 to X.Z.) and funding from the Tsinghua University-Peking University Jointed Center for Life Sciences (to X.L.).

## AUTHOR CONTRIBUTIONS

Yang D performed all of the experiments, and Lin X and Zhao X directed the experiments. Yang D, Zhao X, and Lin X wrote the manuscript.

## ADDITIONAL INFORMATION

The online version of this article (https://doi.org/10.1038/s41423-019-0297-y) contains supplementary material.

**Competing interests:** All institutional and national guidelines for the care and use of laboratory animals were followed. The authors declare no competing interests.

## REFERENCES

1. Li, M. O. & Rudensky, A. Y. T cell receptor signalling in the control of regulatory T cell differentiation and function. *Nat. Rev. Immunol.* **16**, 220–233 (2016).
2. Li M., et al. A wave of Foxp3(+) regulatory T cell accumulation in the neonatal liver plays unique roles in maintaining self-tolerance. *Cell Mol. Immunol.* 2019. [Epub ahead of print].
3. Workman, C. J., Szymczak-Workman, A. L., Collison, L. W., Pillai, M. R. & Vignali, D. A. The development and function of regulatory T cells. *Cell Mol. Life Sci.* **66**, 2603–2622 (2009).
4. Sakaguchi, S., Sakaguchi, N., Asano, M., Itoh, M. & Toda, M. Immunologic self-tolerance maintained by activated T cells expressing IL-2 receptor alpha-chains (CD25). Breakdown of a single mechanism of self-tolerance causes various autoimmune diseases. *J. Immunol.* **155**, 1151–1164 (1995).
5. Hori, S., Nomura, T. & Sakaguchi, S. Control of regulatory T cell development by the transcription factor Foxp3. *Science* **299**, 1057–1061 (2003).
6. Fontenot, J. D., Gavin, M. A. & Rudensky, A. Y. Foxp3 programs the development and function of CD4+CD25+ regulatory T cells. *Nat. Immunol.* **4**, 330–336 (2003).
7. Kumar, P. et al. Critical role of OX40 signaling in the TCR-independent phase of human and murine thymic Treg generation. *Cell Mol. Immunol.* **16**, 138–153 (2019).
8. Nishikawa, H. & Sakaguchi, S. Regulatory T cells in tumor immunity. *Int J. Cancer* **127**, 759–767 (2010).
9. Huehn, J. et al. Developmental stage, phenotype, and migration distinguish naive- and effector/memory-like CD4+ regulatory T cells. *J. Exp. Med.* **199**, 303–313 (2004).
10. Smigiel, K. S. et al. Correction: CCR7 provides localized access to IL-2 and defines homeostatically distinct regulatory T cell subsets. *J. Exp. Med.* **216**, 1965 (2019).
11. Fisson, S. et al. Continuous activation of autoreactive CD4+ CD25+ regulatory T cells in the steady state. *J. Exp. Med.* **198**, 737–746 (2003).
12. Marangoni, F. et al. Tumor tolerance-promoting function of regulatory T cells is optimized by CD28, but strictly dependent on calcineurin. *J. Immunol.* **200**, 3647–3661 (2018).
13. Cretney, E. et al. The transcription factors Blimp-1 and IRF4 jointly control the differentiation and function of effector regulatory T cells. *Nat. Immunol.* **12**, 304–311 (2011).
14. Busse, M., Krech, M., Meyer-Bahlburg, A., Hennig, C. & Hansen, G. ICOS mediates the generation and function of CD4+CD25+Foxp3+ regulatory T cells conveying respiratory tolerance. *J. Immunol.* **189**, 1975–1982 (2012).
15. Lin, W. et al. Regulatory T cell development in the absence of functional Foxp3. *Nat. Immunol.* **8**, 359–368 (2007).
16. Gavin, M. A. et al. Foxp3-dependent programme of regulatory T-cell differentiation. *Nature* **445**, 771–775 (2007).
17. Fontenot, J. D. et al. Regulatory T cell lineage specification by the forkhead transcription factor foxp3. *Immunity* **22**, 329–341 (2005).
18. Levine, A. G., Arvey, A., Jin, W. & Rudensky, A. Y. Continuous requirement for the TCR in regulatory T cell function. *Nat. Immunol.* **15**, 1070–1078 (2014).
19. Luo, C. T. & Li, M. O. Transcriptional control of regulatory T cell development and function. *Trends Immunol.* **34**, 531–539 (2013).
20. Ruan, Q. et al. Development of Foxp3(+) regulatory t cells is driven by the c-Rel enhanceosome. *Immunity* **31**, 932–940 (2009).
21. Oh, H. et al. An NF-kappaB transcription-factor-dependent lineage-specific transcriptional program promotes regulatory T cell identity and function. *Immunity* **47**, 450–465 e455 (2017).
22. Long, M., Park, S. G., Strickland, I., Hayden, M. S. & Ghosh, S. Nuclear factor-kappaB modulates regulatory T cell development by directly regulating expression of Foxp3 transcription factor. *Immunity* **31**, 921–931 (2009).
23. Isomura, I. et al. c-Rel is required for the development of thymic Foxp3+ CD4 regulatory T cells. *J. Exp. Med* **206**, 3001–3014 (2009).
24. Messina, N. et al. The NF-kappaB transcription factor RelA is required for the tolerogenic function of Foxp3(+) regulatory T cells. *J. Autoimmun.* **70**, 52–62 (2016).
25. Sommer, K. et al. Phosphorylation of the CARMA1 linker controls NF-kappaB activation. *Immunity* **23**, 561–574 (2005).
26. Medeiros, R. B. et al. Regulation of NF-kappaB activation in T cells via association of the adapter proteins ADAP and CARMA1. *Science* **316**, 754–758 (2007).
27. Matsumoto, R. et al. Phosphorylation of CARMA1 plays a critical role in T Cell receptor-mediated NF-kappaB activation. *Immunity* **23**, 575–585 (2005).
28. Lee, K. Y., D'Acquisto, F., Hayden, M. S., Shim, J. H. & Ghosh, S. PDK1 nucleates T cell receptor-induced signaling complex for NF-kappaB activation. *Science* **308**, 114–118 (2005).
29. Blonska, M. et al. The CARMA1-Bcl10 signaling complex selectively regulates JNK2 kinase in the T cell receptor-signaling pathway. *Immunity* **26**, 55–66 (2007).
30. Jattani, R. P., Tritapoe, J. M. & Pomerantz, J. L. Cooperative control of caspase recruitment domain-containing protein 11 (CARD11) signaling by an unusual array of redundant repressive elements. *J. Biol. Chem.* **291**, 8324–8336 (2016).
31. Jattani, R. P., Tritapoe, J. M. & Pomerantz, J. L. Intramolecular interactions and regulation of cofactor binding by the four repressive elements in the caspase recruitment domain-containing protein 11 (CARD11) Inhibitory domain. *J. Biol. Chem.* **291**, 8338–8348 (2016).
32. Qiao, Q. et al. Structural architecture of the CARMA1/Bcl10/MALT1 signalosome: nucleation-induced filamentous assembly. *Mol. Cell* **51**, 766–779 (2013).
33. Lin, X. & Wang, D. The roles of CARMA1, Bcl10, and MALT1 in antigen receptor signaling. *Semin Immunol.* **16**, 429–435 (2004).
34. Molinero, L. L. et al. CARMA1 controls an early checkpoint in the thymic development of FoxP3+ regulatory T cells. *J. Immunol.* **182**, 6736–6743 (2009).
35. Brustle, A. et al. MALT1 is an intrinsic regulator of regulatory T cells. *Cell Death Differ.* **24**, 1214–1223 (2017).
36. Campos-Mora, M. et al. CD4+Foxp3+T Regulatory cells promote transplantation tolerance by modulating effector CD4+ T cells in a neuropilin-1-dependent manner. *Front. Immunol.* **10**, 882 (2019).
37. Zheng, Y. et al. Genome-wide analysis of Foxp3 target genes in developing and mature regulatory T cells. *Nature* **445**, 936–940 (2007).
38. Ono, M. et al. Foxp3 controls regulatory T-cell function by interacting with AML1/Runx1. *Nature* **446**, 685–689 (2007).
39. Wilson, C. B., Rowell, E. & Sekimata, M. Epigenetic control of T-helper-cell differentiation. *Nat. Rev. Immunol.* **9**, 91–105 (2009).
40. Szabo, S. J. et al. A novel transcription factor, T-bet, directs Th1 lineage commitment. *Cell* **100**, 655–669 (2000).
41. Koenecke, C. et al. IFN-gamma production by allogeneic Foxp3+ regulatory T cells is essential for preventing experimental graft-versus-host disease. *J. Immunol.* **189**, 2890–2896 (2012).
42. Koch, M. A. et al. The transcription factor T-bet controls regulatory T cell homeostasis and function during type 1 inflammation. *Nat. Immunol.* **10**, 595–602 (2009).
43. Acosta-Iborra, B. et al. Macrophage oxygen sensing modulates antigen presentation and phagocytic functions involving IFN-gamma production through the HIF-1 alpha transcription factor. *J. Immunol.* **182**, 3155–3164 (2009).
44. Lee, J. H., Elly, C., Park, Y. & Liu, Y. C. E3 ubiquitin ligase VHL regulates hypoxia-inducible factor-1alpha to maintain regulatory T cell stability and suppressive capacity. *Immunity* **42**, 1062–1074 (2015).
45. Rosenbaum, M. et al. Bcl10-controlled Malt1 paracaspase activity is key for the immune suppressive function of regulatory T cells. *Nat. Commun.* **10**, 2352 (2019).
46. Di Pilato, M. et al. Targeting the CBM complex causes Treg cells to prime tumours for immune checkpoint therapy. *Nature* **570**, 112–116 (2019).
47. Cheng, L., Deng, N., Yang, N., Zhao, X. & Lin, X. Malt1 protease is critical in maintaining function of regulatory T cells and may be a therapeutic target for antitumor immunity. *J. Immunol.* **202**, 3008–3019 (2019).

48. Ouyang, W. et al. Novel Foxo1-dependent transcriptional programs control T(reg) cell function. *Nature* **491**, 554–559 (2012).
49. Oldenhove, G. et al. Decrease of Foxp3+ Treg cell number and acquisition of effector cell phenotype during lethal infection. *Immunity* **31**, 772–786 (2009).
50. Lu, L. F. et al. Function of miR-146a in controlling Treg cell-mediated regulation of Th1 responses. *Cell* **142**, 914–929 (2010).
51. Ruland, J. & Hartjes, L. CARD-BCL-10-MALT1 signalling in protective and pathological immunity. *Nat. Rev. Immunol.* **19**, 118–134 (2019).
52. O'Rourke D. M., et al. A single dose of peripherally infused EGFRvIII-directed CAR T cells mediates antigen loss and induces adaptive resistance in patients with recurrent glioblastoma. *Sci. Transl. Med.* **9**, pii: eaaa0984 (2017).
53. Maj, T. et al. Oxidative stress controls regulatory T cell apoptosis and suppressor activity and PD-L1-blockade resistance in tumor. *Nat. Immunol.* **18**, 1332–1341 (2017).